Neural Oscillation in Selective Attention and Working Memory

Ruiqi Chen

Department of Machine Intelligence, Peking University

Author Note

Correspondence: crq@pku.edu.cn

Abstract

In this article, I review the computational models for the mechanisms and functions of neural oscillations in selective attention and working memory. First I analyze how bottom-up gamma and top-down beta oscillation may underlie biased competition. Then I review several possible approaches to maintain information in working memory, including persistent firing, theta-gamma coupling, and short term synaptic plasticity. Finally, I introduce the experimental findings and theoretical implications about the temporal response function (TRF), suggesting that it may lead to an integrated description for selective attention and working memory.

Keywords: Neural oscillation, computational model, biased competition, top-down modulation, memory reactivation, theta-gamma coupling, short term plasticity (STP), temporal response function (TRF)

Neural Oscillation, Selective Attention, and Working Memory

Neural oscillation, or the synchronous rhythmic activity of neural networks, is now viewed as the critical “middle ground” linking single-neuron activity to behavior (Buzsáki & Draguhn, 2004). These years, researchers have revealed the intrinsic relation between different cognitive functions and neural oscillations. Here I will focus on two of them: selective attention and working memory.

Selective attention, as defined by the pioneer William James, is “taking possession by the mind, in clear and vivid form, of one out of what may seem several simultaneously possible objects or trains of thought” (James, Burkhardt, Bowers, & Skrupskelis, 1890). Although this area had been investigated for over a century, it was not until recent decades that scientist began to shed light on its neural basis with a fine temporospatial resolution. It was found that attention actually relied on many oscillatory activities. Besides, even the nature of “sustained attention” itself is very likely oscillatory (Jia, Liu, Fang, & Luo, 2017).

Working memory (Baddeley & Hitch, 1974) is the ability to hold and manipulate information for a short period of time, which is crucial for the central execution of human brain. This topic also attracts many theoretical neuroscientist, since it may provide significant insight into the fundamental information encoding mechanism in human brain. Consistent with the experimental findings, many computational models for working memory also demonstrate the importance of neural oscillation in the maintaining of memory.

I will review some most representative models for these two topics first. In the third section, I will analyze the experimental and theoretical efforts to bridge the gap between these two fields, especially through the recent analysis of the brain’s impulse response during sustained attention and working memory.

Neural Oscillation and Selective Attention

Accumulating evidence suggests that selective attention relies on different neural oscillations, especially the synchronization at gamma band and desynchronization at alpha band (Wang, 2010). It is suggested that gamma synchronization indicates the successful encoding of sensory stimulus, while alpha synchronization prevents successful sensory processing (e.g. for distractors). Besides, beta synchronization is believed to support long-range functional coupling (Womelsdorf & Fries, 2007).

Here I will introduce two computational models for the mechanism and computational function of gamma and beta oscillation in selective attention, respectively.

Gamma oscillation and biased competition

Selective attention is often associated with biased competition, where the processing for the attended stimulus dominates that for the unattended stimulus. In a classical experiment, (Moran & Desimone, 1985) found that when two stimuli were presented in the receptive field (RF) of a V4 neuron, the response to the unattended stimulus dramatically reduced, while the V1 response remained unaffected. (Niebur, Koch, & Rosin, 1993) suggested that this mechanism was probably supported by the oscillatory modulation of sensory input and frequency-sensitive higher level processing.

Their model encodes two kinds of features (*red* and *green*) with a group of V1 pyramidal neurons and a group of V4 pyramidal and frequency-sensitive inhibitory neurons. Neurons are uniformly distributed according to their RF, and each V4 neuron receives the input from 100 V1 neurons. V1 neurons make weak connection to V4 pyramidal neurons with different preferred features, strong connection to those with the same feature, and strong connection to interneurons which inhibits the former (See Fig. 1).

Output from V1 is simulated by a Poisson spike chain with mean firing rate λ, which is the summation of a baseline activation and a stimulus-driven activation linear to the overlapping proportion of RF and stimulus. Besides, for the "attended" neurons, the stimulus-driven part is further modulated by a gamma oscillation (e.g. 40Hz), which matches the resonance frequency of the V4 interneurons:

$$\lambda(\mathrm{t}) = \lambda_{\mathrm{bsl}} + \lambda_{max} * overlap(stimulus, RF) * [1 + Asin(\omega t + \phi)]$$

$$\mathrm{A} = A_{max} * overlap(focus\ of\ attention, RF)$$

V4 interneuron is modeled by a RLC circuit selectively amplifying the oscillatory signal from attended area, thus providing stronger inhibition to the unattended. V4 pyramidal neuron is modeled by a HH-equation with a leaky term, a Gaussian noise, and the synaptic input. The synaptic weights are biased towards those favoring the same feature:

$$\tau_{\mathrm{m}} \frac{dV(t)}{dt} = -V(t) - \eta(t) + \rho_e(t)[E_e - V(t)] + \rho_i(t)[E_i - V(t)]$$

$$\frac{d\rho_e(t)}{dt} = -\frac{\rho_e(t)}{\tau_e} + W_e \sum_j \delta(t - t_j) + \frac{W_e}{4} \sum_k \delta(t - t_k)$$

$$\frac{\mathrm{d}\rho_{\mathrm{i}}(t)}{dt} = -\frac{\rho_i(t)}{\tau_i} + W_i \sum_j \delta(t - t_j)$$

The model successfully simulated the result in (Moran & Desimone, 1985). V4 pyramidal neuron's response to attended stimulus was significantly stronger than unattended stimulus, no matter whether the attended stimulus was preferred or not. Frequency domain analysis revealed a peak a 40Hz for the "attended" pyramidal and inhibitory neurons, corresponding to the attentional modulation. Meanwhile, the mean firing rate in V1 remained the same since the modulation was oscillatory.

Beta oscillation and top-down modulation

One of the most influential experiment (Fries, Reynolds, Rorie, & Desimone, 2001) in the field of selective attention demonstrated that neurons with "attention-inside" RF synchronized at gamma band and desynchronize at low frequency (<17Hz) comparing with the nearby "attention-outside" ones. (Lee, Whittington, & Kopell, 2013) tried to explain the data with a model based on top-down beta oscillation.

This model contains two cortical columns, an "attended" one and an "unattended" one, with asynchronous background noise and bottom-up input. Besides, the "attended" column's layer 5 (L5) pyramidal neurons receives top-down beta input (See Fig. 2). The information flow is modulated by L5 neuron in two ways: First, L5 inhibitory output suppresses the inhibition from L4 interneurons to pyramidal neurons; Second, L5 excitatory output strengthens the inhibition to L2/3 neurons in the unattended column.

Local field potential (LFP) was estimated by the summation of synaptic input to pyramidal neurons. The result was in line with (Fries et al., 2001) that attention correlated with enhanced gamma power and reduced beta power in L2/3. Since these neurons output to higher level cortex, the researchers believed that this model implemented a feasible mechanism for attentional gating. Besides, the spike-frequency-coherence was weaker at alpha band but stronger for beta band for attended column comparing with unattended column in deep layers, supporting the distractor-inhibition hypothesis of alpha oscillation.

Neural Oscillation in Working Memory

Working memory has been associated with the persistent firing of neurons for a long time (Wang, 2001), which is often accompanied by the increase of oscillatory power in a certain band. On the other hand, intermittent-bursting-based models became more and more influential

these years (See (Constantinidis et al., 2018) and (Lundqvist, Herman, & Miller, 2018) for a recent debate between them). In this section, I will review some most representative models from both sides, and investigate the source and function of neural oscillation in these models.

Persistent firing

The idea of holding persistent representations in memory can date back to the classical Amari-Hopfield model (Amari, 1972; Hopfield, 1982). In these models, memory item is maintained by the persistent firing of neuron clusters with recurrent connection, which often gives rise to the increase in certain oscillatory activity. Here I will introduce a model from (Wang, 1999).

In this model, a memory item is encoded by a group of densely-connected pyramidal neurons and inhibitory interneurons. The membrane potential of each neuron is modulated by an feedforward input, a leaky current, and the recurrent input through NMDA and AMPA receptors. On top of that, only the pyramidal neurons receive the inhibitory input through GABA receptors:

$$\mathrm{C_m}\frac{dV_m}{dt} = -I_{leaky} - I_{recE} + I_{afferent}\,[-I_{recI}]$$

The AMPA synapse strength is gated by a factor *s*, which represents the proportion of open ion channels. Factor *s* is positively correlated to a short term facilitation (STF) factor *x*, which is modulated by a short term depression (STD) factor *D* representing the available vesicles:

$$\mathrm{I_{AMPA}} = s * g_{AMPA}(V_m - V_E)$$

$$\frac{ds}{dt} = \phi[\alpha_s x(1-s) - \frac{s}{\tau_s}]$$

$$\frac{\mathrm{dx}}{\mathrm{dt}} = \phi[D * \alpha_x \sum_j \delta(t - t_j) - \frac{x}{\tau_x}]$$

$$\frac{\mathrm{dD}}{\mathrm{dt}} = -p_v D \sum_j \delta\left(t - t_j^-\right) + \frac{1 - D}{\tau_D}$$

Roughly speaking, the second equation means that a fixed proportion $\alpha_s x$ of the remaining closed channels will be open after each spike; the third one means that x increases by the amount of released neurotransmitters (available neurotransmitters α_x multiplied by available vesicles *D*) after each spike. And their speeds are modulated by a constant ϕ and different decay time constants. The STD process is described by the utilization of available vesicles with a fixed proportion p_v, and the recovery with time constant τ_D.

The NMDA synapses are modulated with *s* likewise, but also influenced by the extracellular magnesium concentration. The GABA synapses are only modulated by STF but not STD.

Simulation revealed that this network could generate persistent activity with a firing rate of about 40Hz if the recurrent connection was strong enough. Besides, if the excitation is rapid and inhibition is slow, the network could also generate synchronous firing at a frequency of 8-65Hz with different parameters.

Using a modified version of this model, (Compte, Brunel, Goldman-Rakic, & Wang, 2000) successfully simulated the result in the classical experiment about the mnemonic coding of visual space in the monkey's dorsolateral prefrontal cortex (Funahashi, Bruce, & Goldman-Rakic, 1989). They also found that as the NMDA to AMPA ratio decreases, activity became more and more synchronous, with intermittent gamma burst of LFP at a 40Hz rhythm. These simulations indicate that the divergence between persistent firing and intermittent reactivation may be less significant than we have imagined.

Oscillatory dynamics

Although the persistent firing models successfully explained some experimental phenomena, they have a number of apparent drawbacks: from the computation-driven perspective, it is energy-intensive to maintain a high firing rate constantly; from the data-driven perspective, recent electrophysiological experiments revealed more complex dynamics in neural responses with relatively low firing rate during the delay period. Therefore, it is suggested that working memory may incorporate other mechanisms for maintaining a dynamic representation of the elements (Barak & Tsodyks, 2014).

Lisman's theta-gamma coupling model

In a ground-breaking study, (Lisman & Idiart, 1995) presented a model based on theta-gamma coupling and afterdepolarization (ADP). In this model, each item is encoded with a repetitive gamma burst of a cluster of pyramidal cells at a specific theta phase, so that the items are sequentially reactivated in the same order as they are encoded. Each pyramidal cell is assumed to receive a subthreshold oscillatory input at theta band, a suprathreshold informative input, and a pooled feedback inhibition which implemented a winner-take-all mechanism and thus dividing the theta cycle into gamma windows. Besides, the afterdepolarization current increases the neurons' excitability right after the spike, enabling them to spike repetitively in a theta rhythm. Therefore, $\tau_{\mathrm{v}} \frac{dV_i(t)}{dt} = V^{rest} - V_i(t) + V^{inh}(t) + V^{osc}(t) + V_i^{ADP}(t)$. The inhibitory feedback is modeled as the integrative response for a series of excitatory inputs: $V^{inh}(t) = \sum_t \alpha(t - tn)$, where $\alpha(\mathrm{t}) = A * \frac{t}{\tau} * \exp(1 - \frac{\mathrm{t}}{\tau})$. The ADP is also modeled as an alpha function with time constant approximately equal to a theta cycle. Simulation demonstrated that this network could robustly store an ordered sequence of 7 ± 2 items, and old items would be lost if overloaded (See Fig. 3).

This theory was corroborated by many neurobiological findings. Subthreshold theta oscillation was first found in the layer II neurons in the entorhinal cortex (Alonso & Llinás, 1989), and theta oscillation of the LFP was very prominent in the hippocampus (Buzsáki, 2002). More interestingly, these theta oscillations are often temporally nested by gamma oscillations (Bragin et al., 1995; Lisman & Jensen, 2013). Besides, it is widely recognized that hippocampus is crucial for learning and memory, and its input mainly comes from the entorhinal cortex. Considering the converging evidence, Jensen and Lisman updated this model in 2005, suggesting that the entorhinal cortex may implement a theta-gamma coupling mechanism as a working memory buffer, which receives information from the neocortex and sends it to hippocampus for learning and long term memory formation (Jensen & Lisman, 2005). The updated model incorporated more biological details to elaborate the encoding and decoding process. First, it suggested that the working memory buffer could compress the interval between memory items to the time window of long term potentiation (LTP), which offered a possible mechanism for the learning of sequence with behavioral time scale. Second, the memorized items could be retrieved through chaining activation, probably by phase precession of the hippocampus theta rhythm (O'Keefe & Recce, 1993).

The most attractive feature of this model is that it successfully explains two classical findings in psychology. First, the capacity of short term (working) memory was estimated to be 7 ± 2 (G. A. Miller, 1956), corresponding to the maximum number of gamma windows in a theta cycle. Although this number was correct to 4 recently (Cowan, 2001), Lisman's model still provided us a creative approach to understand the limit of human information processing. Second, the cycle period of informative gamma oscillation was approximately equal to the memory scanning time for each item in Sternberg paradigm (Sternberg, 1966). Scalp EEG or

intracranial recordings on human also provided some evidence about the theta-gamma coupling in hippocampus during working memory experiments (Axmacher et al., 2010; Heusser, Poeppel, Ezzyat, & Davachi, 2016).

Tsodykes' synaptic plasticity model

(Mongillo, Barak, & Tsodyks, 2008) established a model where each memory item is encoded by a cluster of neurons, and competes with each other through pooled feedback inhibition. The fluctuation of STP and STD level of the pyramidal-pyramidal synapse leads to the repetitive sequential reactivation of memory trace. To be specific, each pyramidal neuron receives a Gaussian random input $\mathrm{I_i^{ext}}(t)$ and the recurrent input $\mathrm{I_i^{rec}}(t)$, which is the summation of spikes weighted by the synaptic strength $\hat{\mathrm{J}}_{\mathrm{ij}}(\mathrm{t})$:

$$\tau_{\mathrm{m}} \frac{dV}{dt} = -V_i + \mathrm{I_i^{ext}}(t) + \mathrm{I_i^{rec}}(t)$$

$$\mathrm{I_i^{ext}}(t) = \mu_{ext} + \sigma_{ext}(t)\eta_i^{ext}(t)$$

$$\mathrm{I_i^{rec}}(t) = \sum_j \hat{J}_{ij}(t) \sum_k \delta(t - t_k^j - D_{ij})$$

Here $\mathrm{D_{ij}}$ is the synaptic delay and t_k^j is the onset time of the *k*-th spike for neuron *j*. The synaptic connection weight is modulated by the portion of available neurotransmitters *x* and the "utilization factor" *u*, which may reflect the portion of opening calcium channels. Similar to (Wang, 1999), short term depression is represented by the release of neurotransmitters (thus the decrease of *x*), and facilitation is associated to the opening of a constant ratio (denoted as *U*) of closed calcium channels (thus the increase of *u*):

$$\hat{J}_{ij}(t) = J_{ij} * u\big(t - D_{ij}\big) * x\big(t - D_{ij}\big)$$

$$\frac{dx_j(t)}{dt} = \frac{1 - x_j(t)}{\tau_{\mathrm{D}}} - u_j(t)x_j(t) \sum_k \delta(t - t_k^j)$$

$$\frac{du_j(t)}{dt} = \frac{U - u_j(t)}{\tau_F} + U[1 - u_j(t)] \sum_k \delta(t - t_k^j)$$

Simulation shows that this network can generate either oscillatory or asynchronous continuous firing given different external input. In the oscillatory state, items can be reactivated sequentially for several cycles (See Fig. 4). A recent analysis (Mi, Katkov, & Tsodyks, 2017) revealed more interesting behavioral implications of this model. The authors found that this model could simulate the recency and primacy effect if the items were presented in a very fast speed. Besides, the working memory capacity was linear to $\frac{\tau_d}{\tau_m}$. The most intriguing finding was that the sequence can be segmented by modulating the external input with a square wave, providing a possible explanation of the chunking effect in working memory experiments.

Lundqvist's model

(Lundqvist, Herman, & Lansner, 2011) established an elaborated model to explain the increase of gamma power and decrease of alpha/beta power common in working memory experiments (Jensen & Tesche, 2002; Lundqvist, Herman, Warden, Brincat, & Miller, 2018; Lundqvist et al., 2016). This network is organized into nine hypercolumns, each containing 7×7 minicolumns. 30 pyramidal neurons spread out along the *z* axis of each minicolumn, with 1 basket cell and 2 regular spiking nonpyramidal (RSNP) cells in the middle position, mimicking the layer II/III neurons. The RSNP cells have inhibitory connection with the pyramidal cells within the same minicolumn, and the basket cells provide feedback inhibition to the whole hypercolumn, both with a connectivity probability of 70%.

Each memory item is encoded as 9 attributes with 49 possible value for each attribute, namely, 9 minicolumns each in one hypercolumn. Pyramidal cells project to other pyramidal cells within the same minicolumn with a probability of 25%, and to those encoding other

attributes (in other hypercolumns) of the same memory item with a probability of 30%, both facilitating the activation of memory trace. Besides, they project to the eight nearest basket cells with a probability of 70%, and to RSNP cells in other hypercolumns with a probability of 30% if the targeted minicolumn encodes a different item, both suppressing the activation of other items (See Fig. 5A). Besides, each layer II/III pyramidal neuron receives the baseline activation from layer IV neuron in the same minicolumn with 50% connectivity, and a noise from a Poisson spike train.

Simulation shows that this network can either be a ground state with alpha/beta band spontaneous firing or a repetitive memory activation state, with the burst rate in gamma range and lasting time in theta range (See Fig. 5B). More importantly, the researchers simulated the LFP with the mean soma potential within local range, and revealed the increase of theta/gamma power and decrease of alpha/beta power as memory load increases. The model also predicts the phase-amplitude coupling and phase-locking between theta and gamma band, which are often found in experimental data (Axmacher et al., 2010; Belluscio, Mizuseki, Schmidt, Kempter, & Buzsáki, 2012).

One of the most important feature of this model is that it maintains the periodical gamma burst without replaying the whole memory list in every theta cycle. This is not only energy-efficient but also more biologically plausible. For example, the number of nested gamma bursts within each theta cycle was shown to be constant as the memory load increases (Axmacher et al., 2010), contradictory with Lisman's model but compatible with the current one. Besides, the model predicts that the gamma bursts are not periodic and interrupted by alpha/beta bursts representing the baseline state, which was proved by a later experiment (Lundqvist et al., 2016). However, this model fails to explain the memory of order since different items are not

reactivated sequentially. In a follow-up proposal, (E. K. Miller, Lundqvist, & Bastos, 2018) suggested that manipulation of the memory content, including reordering and sequencing, may lie in the top-down modulation of the superficial gamma activation through the alpha/beta oscillation in deeper cortical layers.

Integrated Model for the "Focus of Mind"

We have reviewed the computational functions of neural oscillations in attention and working memory respectively, and it will be interesting to analyze the similarity between these two mental process and the underlying mechanisms. "Focus of attention" is sometimes recognized as a subset of working memory (Cowan, 1999), and both processes are often associated with the decrease of alpha energy and increase of gamma energy. Besides, recent analyses illustrated that the dynamics of alpha band dynamics of the temporal response function (TRF) indicated both the shifting of attention and replay of memorized items (Huang, Jia, Han, & Luo, 2018; Jia et al., 2017; Vanrullen & MacDonald, 2012). Therefore, it is suggested that attention and working memory may share a same neural substrate (Wang, 2010).

Combining attention and working memory

(Ardid, Wang, Gomez-Cabrero, & Compte, 2010) introduced a model for the working memory and selective attention of stimulus motion. The model is composed of two rings of neurons representing the working memory buffer (e.g. PFC) and sensory processing area (e.g. MT) respectively. Each network contains 1/5 inhibitory interneurons and 4/5 excitatory neurons, densely connected and arranged according to their preferred orientation. Excitatory-excitatory connections are weighted by a Gaussian function according to the difference in preferred orientation, so as to create a continuous attractor (Amari, 1977). Interareal connections are

specified likewise with different parameters, enabling the bottom-up registration and top-down modulation (See Fig. 6).

The researchers tried to simulate a delay-matching-to-sample task with this model. When stimulus moves, a constant current and a gamma oscillation will be injected to MT, mimicking the sensory input from V1. This current is tuned so that the activation profile is in a bell shape similar to that of the interareal connection. PFC receives a baseline underthreshold activation so that it will be activated if MT provides a strong input, and the orientation will be registered in working memory. Likewise, the attractor state of PFC will enhance the activity of the corresponding MT area though top-down connections, mimicking the attentional effect. Researchers estimated the LFP by the summation of EPSCs from a group of nearby neurons. It turned out that PFC's attentional modulation significantly enhances the gamma oscillation in MT while keeping the irregular spiking intact. This model successfully replicated the result of real electrophysiological experiments, and bridged the gap between irregular neuron spikes and synchronized LTP oscillation.

Implications of the "alpha echo"

Up to now, I have only discussed the spontaneous neural oscillation. However, recent experiments reveled another kind of oscillation: the brain's impulse response, or TRF. By definition, TRF should mimic the traditional event-related-potential (ERP) (Lalor, Pearlmutter, Reilly, McDarby, & Foxe, 2006). However, ERP is computed by averaging the response to a single impulse, while TRF is estimated by regression between continuous input and response. TRF actually contains more information about the nonlinear integration of past input, which is missing in ERP. Experiments also illustrated that although the early component of TRF resembled ERP, the late component turned out to be much more oscillatory (Vanrullen &

MacDonald, 2012). This result proves that the brain cannot be assumed as a linear time invariant (LTI) system even in the most basic sensory processing. However, this leads to a paradox since the computation, and even the concept of TRF was also based on the LTI presumption (the same for ERP). Nevertheless, TRF still enables us to "dig into" the brain under a semi-real situation, since the sensory system is aimed for continuous changes rather than constant stimuli, which are often used in ERP experiments.

TRF and cognitive functions

TRF has been showed to be modulated by attention in both auditory cocktail party paradigm (Zion Golumbic et al., 2013) and visual covert attention paradigm (cuing task) (Jia, Fang, & Luo, 2019; Jia et al., 2017; Vanrullen & MacDonald, 2012). (Jia et al., 2017) analyzed the dynamics of the alpha band TRF. They found that attention was associated with the decrease in alpha band power in 0-200ms and a rebound in the following 200ms, if given a 100% validity cue. As the validity of the cue decreases, participants had to distribute their attention more equally on both the cued and uncued item, and the alpha power difference between the attended and unattended TRF became more and more oscillatory, repetitively changing sign in every 200ms, thus suggesting the "sequential sampling" of visual stimulus during sustained attention (See Fig. 7A).

TRF is also related to the activation of items in working memory. (Huang et al., 2018) found that the memory items (e.g. tilted bars) could be bound to irrelevant features (e.g. color), and the TRF of a "tag" with this feature could reveal the delayed-period dynamics of the corresponding item. They found that in one-item working memory, the "working-memory-relevant TRF" (denoted as WM-TRF) had stronger alpha power around 200ms-400ms, similar to the effect of attention. When the number of memory item increased, the difference in WM-TRF

and NWM-TRF's alpha power also mimicked the result in (Jia et al., 2017), except that the first 200ms was characterized by increased alpha rather than decrease (See Fig. 7B). A more interesting result is the comparison between different items. It was shown that the relative alpha power between item-relevant TRF was also oscillatory, with a reversed temporal profile (the most recently encoded one being in advance, see Fig. 7C), which was related to the strength of recency effect in later memory task. (Li, Huang, Han, & Luo, 2019) reports a more intriguing result, showing that the primacy and recency effect can be distorted by the alpha-synchronized memory-relevant "tags", further stressing the implication of TRF in the sequential working memory.

Computational basis of TRF

Characterized by the oscillatory modulation of alpha band power, does TRF reveal the shared neural mechanism underlying attention and working memory? Unfortunately, to my best knowledge, no computational models have been raised to answer this question. Here, I would like to share my opinion and hypothesis about the neural basis of TRF and its implication in attention and working memory.

First, the oscillatory TRF can probably be explained by a model similar to the oscillation-based models for working memory, which often generate repetitive neural activities after activated by a strong input, namely, an impulse.

Second, a model with a working memory network and a sensory network can explain the inconsistency in the current data. A challenging problem about TRF was that the first 200ms seems to show different pattern with the rest of TRF, and high variability among tasks. For example, both using the cuing task with 100% validity, (Vanrullen & MacDonald, 2012) reported no attentional effect in the first 200ms while (Jia et al., 2017) reported decrease in

alpha; both incorporating relevant and irrelevant stimuli, (Huang et al., 2018) and (Jia et al., 2017) reported similar TRF except reversed trend in the first 200ms. This discrepancy can be explained by the fact that TRF mimics visual ERP, especially in the first 200ms (Lalor et al., 2006). Due to the poor spatial resolution of EEG, the occipital ERP/TRF may overlap with the parietal TRF and distort its temporal profile.

A recent experiment proves that selective attention actually involved two alpha band TRF component (Jia et al., 2019). One was at the posterior parietal cortex and negatively modulated by attention, representing the top-down inhibition of irrelevant stimulus; one was at the contralateral occipital cortex and positively modulated by attention, representing the sensory processing. Besides, in the working memory experiment, after ruling out the sensory effect (by subtracting the response to NWM item from that to two WM items), the alpha energy difference in TRF was also shown to be rhythmically fluctuated (Huang et al., 2018) (See Fig. 7C).

Third, working memory cannot be simply viewed as “internal attention”. In aforementioned working memory experiments, higher memory strength (e.g. stronger recency effect) was associated with higher alpha power in the first 200ms (e.g. the second item relative to the first item), in contrast to the attentional effect of weaker parietal alpha. Either that the working memory items are stored in the sensory area, or the temporal organization of memory sequence involves a different kind of top-down modulation.

Here I adopt the second explanation, as is also suggested by (E. K. Miller et al., 2018). Therefore, a complete model for TRF should have an occipital sensory part (e.g. V1) and a parietal control part (e.g. intraparietal sulcus (IPS), which is shown to be important in both visuospatial attention and working memory), similar to the idea in (Ardid et al., 2010). In order to explain the experimental data, it would be reasonable to implement a working memory buffer

similar to the one in (Lundqvist et al., 2011), representing each item as a conjunction of spatial location, orientation, color, and saliency. In attentional experiments, a top-down current will be injected to the desired "location" minicolumn, representing selective attention. Therefore, the representation of the attended stimulus (with its "location" attribute already registered) will be more easily activated given an impulse input (e.g. activating the "saliency" minicolumn), leading to stronger gamma burst and greater decrease of "default" alpha/beta power in the first 200ms. As this activation fades out, alpha takes place again and will be interrupted by the next round of gamma burst, similar to the 2.5Hz oscillation in alpha amplitude found in experiment. Similarly, for the working memory experiment, as the memory trace reactivates in this buffer, item-relevant "color" minicolumns are also activated, leading to stronger response (lower alpha) for item-relevant tag (with the same "color" attribute) comparing with item-irrelevant tag. Besides, the ordering of memory items are mediated through another top-down process, probably alpha/beta oscillatory input (E. K. Miller et al., 2018), which may explain the "fast backward replay" in (Huang et al., 2018). As for the sensory part, it was shown that a cortical-column-based model (Jansen & Rit, 1995) can mimic the "alpha echo" in (Vanrullen & MacDonald, 2012) very closely (See Fig. 8). Therefore, the parietal alpha may modulate the sensory alpha through connections between the corresponding minicolumns in IPS and V1, consistent with the result in (Jia et al., 2019).

Conclusion

In this article, I review the computational models about the function of neural oscillation in attention and working memory. In both mental processes, gamma oscillation is related to the information encoding, beta relating to top-down modulation, alpha relating to distractor inhibition, and theta relating to temporal organization. Besides, recent advance in TRF also

reveals their analogy in temporal dynamics. I am looking forward to more theoretic analysis about the underlying mechanism for these two processes, as well as the essential relationship between them.

Reference

Alonso, A., & Llinás, R. R. (1989). Subthreshold Na+-dependent theta-like rhythmicity in stellate cells of entorhinal cortex layer II. *Nature*, *342*(6246), 175–177. https://doi.org/10.1038/342175a0

Amari, S. I. (1972). Learning patterns and pattern sequences by self-organizing nets of threshold elements. *IEEE Transactions on Computers*, *C–21*(11), 1197–1206. https://doi.org/10.1109/T-C.1972.223477

Amari, S. I. (1977). Dynamics of pattern formation in lateral-inhibition type neural fields. *Biological Cybernetics*, *27*(2), 77–87. https://doi.org/10.1007/BF00337259

Ardid, S., Wang, X. J., Gomez-Cabrero, D., & Compte, A. (2010). Reconciling coherent oscillation with modulation of irregular spiking activity in selective attention: Gamma-range synchronization between sensory and executive cortical areas. *Journal of Neuroscience*, *30*(8), 2856–2870. https://doi.org/10.1523/JNEUROSCI.4222-09.2010

Axmacher, N., Jensen, O., Elger, C. E., Fell, J., Henseler, M. M., Weinreich, I., … Fell, J. (2010). Cross-frequency coupling supports multi-item working memory in the human hippocampus. *Proceedings of the National Academy of Sciences*, *107*(7), 3228–3233. https://doi.org/10.1073/pnas.0911531107

Baddeley, A. D., & Hitch, G. J. (1974). Working memory. *Psychology of Learning and Motivation - Advances in Research and Theory*, *8*(C), 47–89. https://doi.org/10.1016/S0079-7421(08)60452-1

Barak, O., & Tsodyks, M. (2014, April). Working models of working memory. *Current Opinion in Neurobiology*, Vol. 25, pp. 20–24. https://doi.org/10.1016/j.conb.2013.10.008

Belluscio, M. A., Mizuseki, K., Schmidt, R., Kempter, R., & Buzsáki, G. (2012). Cross-

frequency phase-phase coupling between theta and gamma oscillations in the hippocampus. *Journal of Neuroscience, 32*(2), 423–435. https://doi.org/10.1523/JNEUROSCI.4122-11.2012

Bragin, A., Jando, G., Nadasdy, Z., Hetke, J., Wise, K., & Buzsáki, G. (1995). Gamma (40-100 Hz) oscillation in the hippocampus of the behaving rat. *Journal of Neuroscience, 15*(1 I), 47–60. https://doi.org/10.1523/jneurosci.15-01-00047.1995

Buzsáki, G. (2002, January 31). Theta oscillations in the hippocampus. *Neuron*, Vol. 33, pp. 325–340. https://doi.org/10.1016/S0896-6273(02)00586-X

Buzsáki, G., & Draguhn, A. (2004, June 25). Neuronal oscillations in cortical networks. *Science*, Vol. 304, pp. 1926–1929. https://doi.org/10.1126/science.1099745

Compte, A., Brunel, N., Goldman-Rakic, P. S., & Wang, X.-J. (2000). Synaptic Mechanisms and Network Dynamics Underlying Spatial Working Memory in a Cortical Network Model. *Cerebral Cortex, 10*(9), 910–923. https://doi.org/10.1093/cercor/10.9.910

Constantinidis, C., Funahashi, S., Lee, D., Murray, J. D., Qi, X. L., Wang, M., & Arnsten, A. F. T. (2018). Persistent spiking activity underlies working memory. *Journal of Neuroscience, 38*(32), 7020–7028. https://doi.org/10.1523/JNEUROSCI.2486-17.2018

Cowan, N. (1999). An Embedded-Processes Model of Working Memory. In *Models of Working Memory* (pp. 62–101). https://doi.org/10.1017/cbo9781139174909.006

Cowan, N. (2001). The magical number 4 in short-term memory: A reconsideration of mental storage capacity. *Behavioral and Brain Sciences, 24*(1), 87–114. https://doi.org/10.1017/S0140525X01003922

Fries, P., Reynolds, J. H., Rorie, A. E., & Desimone, R. (2001). Modulation of oscillatory neuronal synchronization by selective visual attention. *Science, 291*(5508), 1560–1563.

https://doi.org/10.1126/science.1055465

Funahashi, S., Bruce, C. J., & Goldman-Rakic, P. S. (1989). Mnemonic coding of visual space in the monkey's dorsolateral prefrontal cortex. *Journal of Neurophysiology*, *61*(2), 331–349. https://doi.org/10.1152/jn.1989.61.2.331

Heusser, A. C., Poeppel, D., Ezzyat, Y., & Davachi, L. (2016). Episodic sequence memory is supported by a theta–gamma phase code. *Nature Neuroscience*, *19*(10), 1374–1380. https://doi.org/10.1038/nn.4374

Hopfield, J. J. (1982). Neural networks and physical systems with emergent collective computational abilities. *Proceedings of the National Academy of Sciences of the United States of America*, *79*(8), 2554–2558. https://doi.org/10.1073/pnas.79.8.2554

Huang, Q., Jia, J., Han, Q., & Luo, H. (2018). Fast-backward replay of sequentially memorized items in humans. *ELife*, *7*. https://doi.org/10.7554/eLife.35164

James, W., Burkhardt, F., Bowers, F., & Skrupskelis, I. K. (1890). *The principles of psychology* (Vol. 1). Macmillan London.

Jansen, B. H., & Rit, V. G. (1995). Electroencephalogram and visual evoked potential generation in a mathematical model of coupled cortical columns. *Biological Cybernetics*, *73*(4), 357–366. https://doi.org/10.1007/BF00199471

Jensen, O., & Lisman, J. E. (2005). Hippocampal sequence-encoding driven by a cortical multi-item working memory buffer. *Trends in Neurosciences*, *28*(2), 67–72. https://doi.org/10.1016/j.tins.2004.12.001

Jensen, O., & Tesche, C. D. (2002). Frontal theta activity in humans increases with memory load in a working memory task. *European Journal of Neuroscience*, *15*(8), 1395–1399. https://doi.org/10.1046/j.1460-9568.2002.01975.x

Jia, J., Fang, F., & Luo, H. (2019). Selective spatial attention involves two alpha-band components associated with distinct spatiotemporal and functional characteristics. *NeuroImage*, *199*, 228–236. https://doi.org/10.1016/j.neuroimage.2019.05.079

Jia, J., Liu, L., Fang, F., & Luo, H. (2017). Sequential sampling of visual objects during sustained attention. *PLoS Biology*, *15*(6), e2001903. https://doi.org/10.1371/journal.pbio.2001903

Lalor, E. C., Pearlmutter, B. A., Reilly, R. B., McDarby, G., & Foxe, J. J. (2006). The VESPA: A method for the rapid estimation of a visual evoked potential. *NeuroImage*, *32*(4), 1549–1561. https://doi.org/10.1016/j.neuroimage.2006.05.054

Lee, J. H., Whittington, M. A., & Kopell, N. J. (2013). Top-Down Beta Rhythms Support Selective Attention via Interlaminar Interaction: A Model. *PLoS Computational Biology*, *9*(8). https://doi.org/10.1371/journal.pcbi.1003164

Li, J., Huang, Q., Han, Q., & Luo, H. (2019). Manipulating serial replay during memory retention rapidly alters human sequence memory. *BioRxiv*, 631531. https://doi.org/10.1101/631531

Lisman, J. E., & Idiart, M. A. P. (1995). Storage of 7 ± 2 short-term memories in oscillatory subcycles. *Science*, *267*(5203), 1512–1515. https://doi.org/10.1126/science.7878473

Lisman, J. E., & Jensen, O. (2013). The Theta-Gamma Neural Code. *Neuron*, *77*(6), 1002–1016. https://doi.org/10.1016/j.neuron.2013.03.007

Lundqvist, M., Herman, P., & Lansner, A. (2011). Theta and gamma power increases and alpha/beta power decreases with memory load in an attractor network model. *Journal of Cognitive Neuroscience*, *23*(10), 3008–3020. https://doi.org/10.1162/jocn_a_00029

Lundqvist, M., Herman, P., & Miller, E. K. (2018). Working memory: Delay activity, yes!

persistent activity? maybe not. *Journal of Neuroscience*, *38*(32), 7013–7019. https://doi.org/10.1523/JNEUROSCI.2485-17.2018

Lundqvist, M., Herman, P., Warden, M. R., Brincat, S. L., & Miller, E. K. (2018). Gamma and beta bursts during working memory readout suggest roles in its volitional control. *Nature Communications*, *9*(1). https://doi.org/10.1038/s41467-017-02791-8

Lundqvist, M., Rose, J., Herman, P., Brincat, S. L., Buschman, T. J., & Miller, E. K. (2016). Gamma and Beta Bursts Underlie Working Memory. *Neuron*, *90*(1), 152–164. https://doi.org/10.1016/j.neuron.2016.02.028

Mi, Y., Katkov, M., & Tsodyks, M. (2017). Synaptic Correlates of Working Memory Capacity. *Neuron*, *93*(2), 323–330. https://doi.org/10.1016/j.neuron.2016.12.004

Miller, E. K., Lundqvist, M., & Bastos, A. M. (2018, October 24). Working Memory 2.0. *Neuron*, Vol. 100, pp. 463–475. https://doi.org/10.1016/j.neuron.2018.09.023

Miller, G. A. (1956). The magical number seven, plus or minus two: some limits on our capacity for processing information. *Psychological Review*, *63*(2), 81–97. https://doi.org/10.1037/h0043158

Mongillo, G., Barak, O., & Tsodyks, M. (2008). Synaptic Theory of Working Memory. *Science*, *319*(5869), 1543–1546. https://doi.org/10.1126/science.1150769

Moran, J., & Desimone, R. (1985). Selective attention gates visual processing in the extrastriate cortex. *Science*, *229*(4715), 782–784. https://doi.org/10.1126/science.4023713

Niebur, E., Koch, C., & Rosin, C. (1993). An oscillation-based model for the neuronal basis of attention. *Vision Research*, *33*(18), 2789–2802. https://doi.org/10.1016/0042-6989(93)90236-P

O'Keefe, J., & Recce, M. L. (1993). Phase relationship between hippocampal place units and the

EEG theta rhythm. *Hippocampus*, *3*(3), 317–330. https://doi.org/10.1002/hipo.450030307

Sternberg, S. (1966). High-speed scanning in human memory. *Science*, *153*(3736), 652–654. https://doi.org/10.1126/science.153.3736.652

Vanrullen, R., & MacDonald, J. S. P. (2012). Perceptual echoes at 10 Hz in the human brain. *Current Biology*, *22*(11), 995–999. https://doi.org/10.1016/j.cub.2012.03.050

Wang, X. J. (1999). Synaptic basis of cortical persistent activity: The importance of NMDA receptors to working memory. *Journal of Neuroscience*, *19*(21), 9587–9603. https://doi.org/10.1523/jneurosci.19-21-09587.1999

Wang, X. J. (2001, August 1). Synaptic reverberation underlying mnemonic persistent activity. *Trends in Neurosciences*, Vol. 24, pp. 455–463. https://doi.org/10.1016/S0166-2236(00)01868-3

Wang, X. J. (2010, July). Neurophysiological and computational principles of cortical rhythms in cognition. *Physiological Reviews*, Vol. 90, pp. 1195–1268. https://doi.org/10.1152/physrev.00035.2008

Womelsdorf, T., & Fries, P. (2007, April). The role of neuronal synchronization in selective attention. *Current Opinion in Neurobiology*, Vol. 17, pp. 154–160. https://doi.org/10.1016/j.conb.2007.02.002

Zion Golumbic, E. M., Ding, N., Bickel, S., Lakatos, P., Schevon, C. A., McKhann, G. M., … Schroeder, C. E. (2013). Mechanisms underlying selective neuronal tracking of attended speech at a “cocktail party.” *Neuron*, *77*(5), 980–991. https://doi.org/10.1016/j.neuron.2012.12.037

Figures

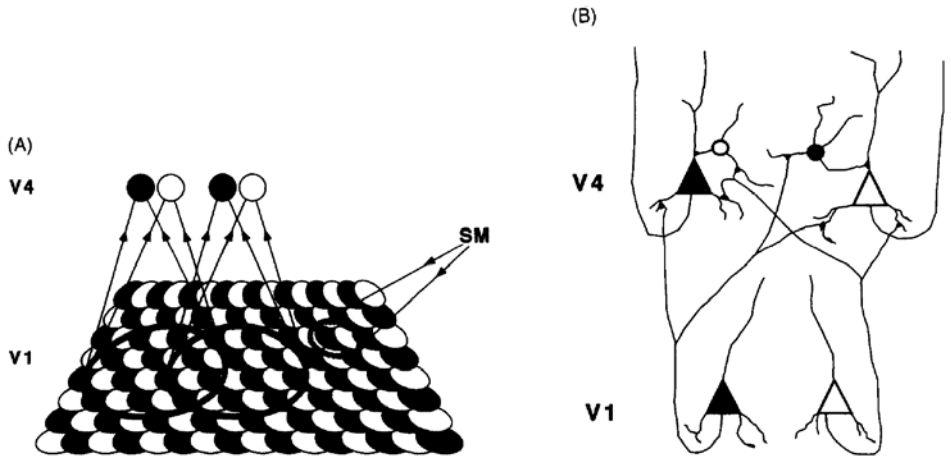

Figure 1. The attention network from (Niebur et al., 1993). Black and white neurons prefer feature *red* and *green* respectively. (**A**) Neurons are arranged consecutively according to their RF. SM indicates the area modulated by the saliency map (attention and gamma oscillation). (**B**) Triangles indicates pyramidal neurons and circles indicates inhibitory interneurons. Connection between neurons with the same preferred feature is stronger than that with different features.

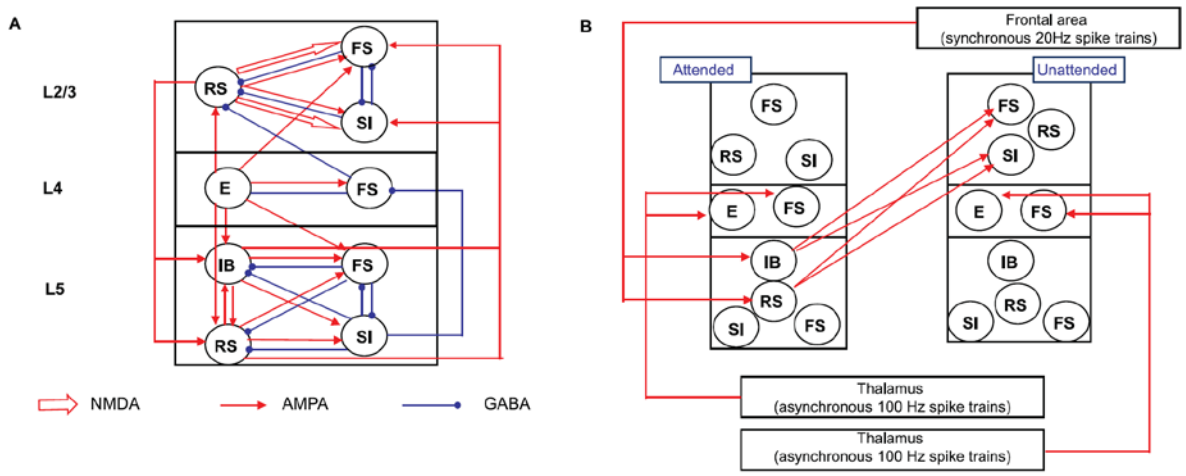

Figure 2. The top-down beta modulation model for selective attention in (Lee et al., 2013). Neuron types: RS, regular spiking pyramidal neurons; FS, fast spiking neurons; SI, slow inhibition neurons; E, excitatory neurons; IB, intrinsic bursting pyramidal neurons. The intercolumnar connection pattern between L5 and L2/3 are identical to the corresponding intracolumnar one but with 50% weight.

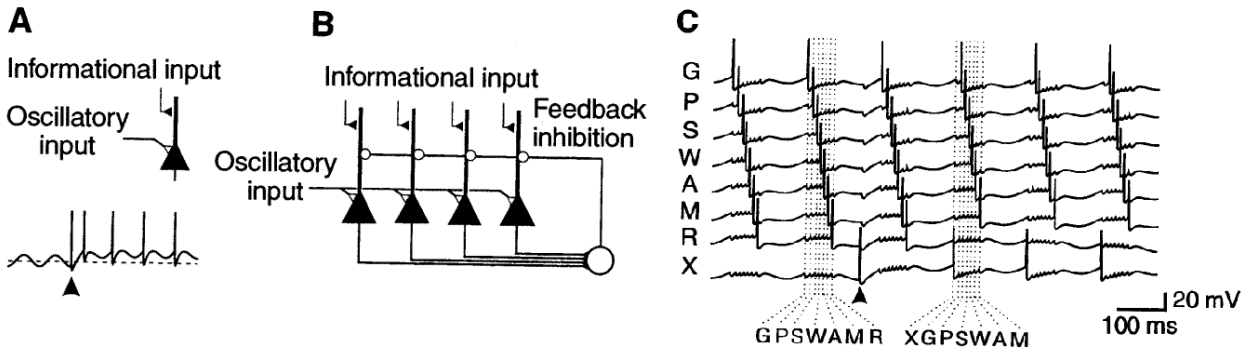

Figure 3. Theta-gamma coupling model from (Lisman & Idiart, 1995). (**A**) ADP current drives the neuron to fire rhythmically. (**B**) The memory network with four pyramidal neurons encoding four stimuli and inhibited by a same interneuron. (**C**) Simulation of the memory encoding. The network can store 7 stimuli with a theta rhythm, but adding the eighth stimulus ("X") leads to the loss of previous information ("R").

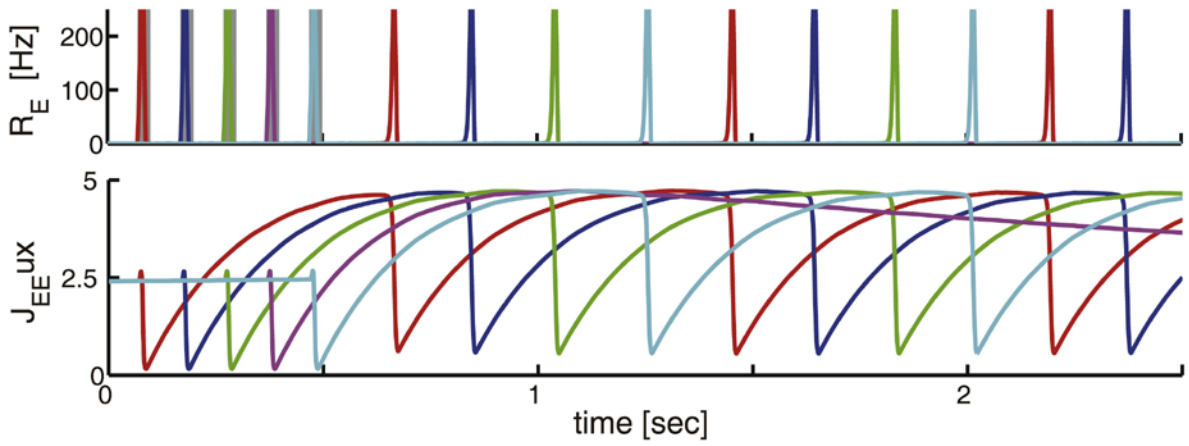

Figure 4. Tsodykes' synaptic model for working memory (Mi et al., 2017; Mongillo et al., 2008). Memories are reactivated at a theta rhythm sequentially.

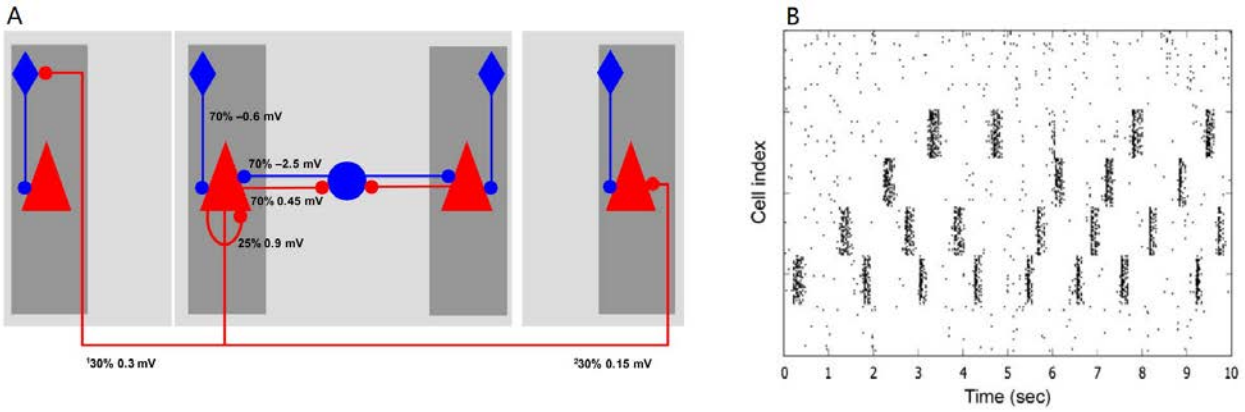

Figure 5. Lundqvist's model (Lundqvist et al., 2011). (**A**) Illustration of the connections. Light square indicates hypercolumn and dark square indicates minicolumn. Blue circles: basket cells; Blue rhombs: RSNP cells; Red triangle: pyramidal cells. [1]If encoding the same pattern, otherwise none. [2]If encoding the same pattern, otherwise none. (**B**) Rastergram for neuron spiking with four memory items. Items are reactivated repetitively and shut down after about 200ms.

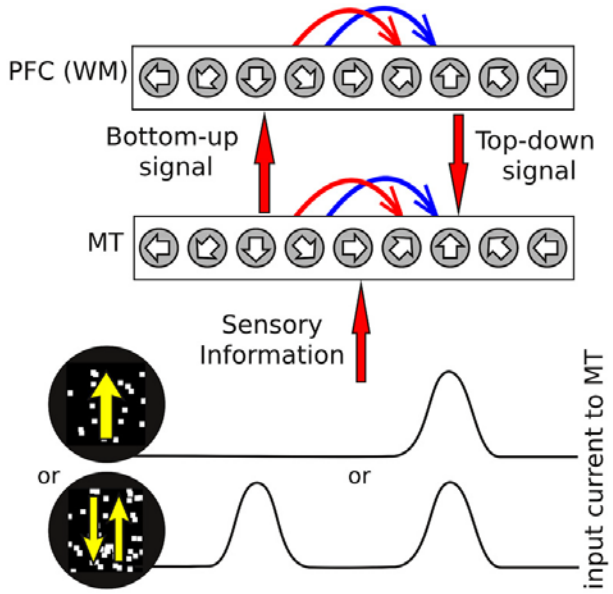

Figure 6. Integrated model for attention and working memory (Ardid et al., 2010). Neurons are labeled by their preferred orientation. Blue arrows indicate inhibition and red ones indicate activation.

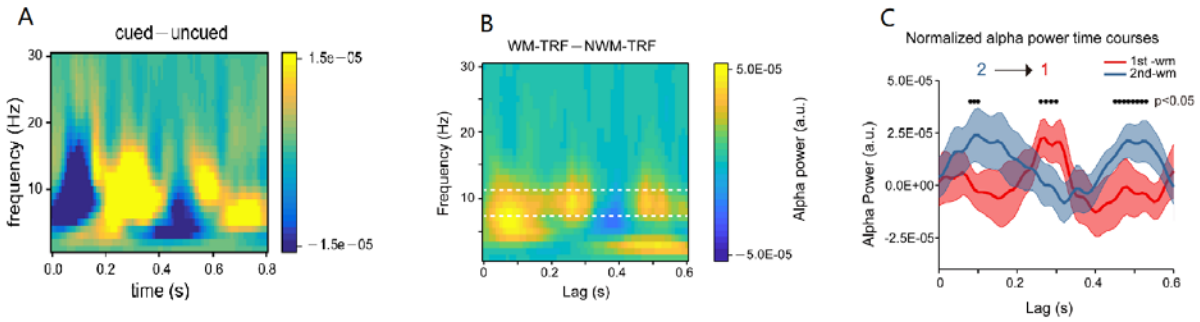

Figure 7. TRF alpha power in selective attention and working memory (Huang et al., 2018; Jia et al., 2017). (**A**) TRF alpha power in a Posner cuing task with 50% cue validity. (**B**) TRF alpha power difference between stimulus-related and unrelated tags, in the delay period of a working memory task. (**C**) Normalized TRF alpha power for tags related to each stimulus.

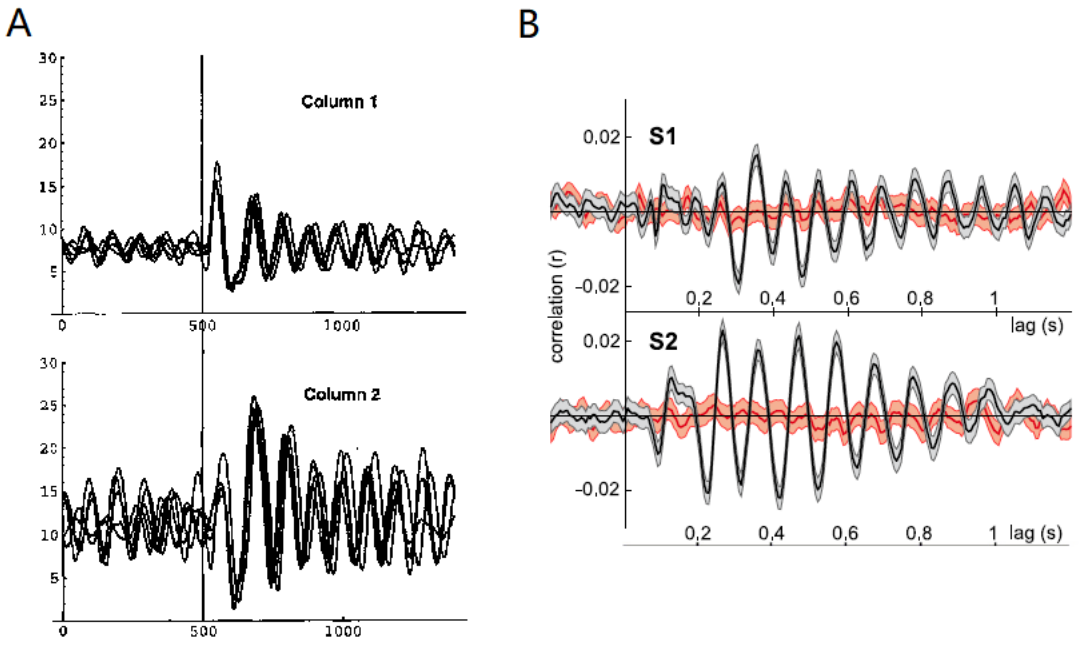

Figure 8. A column-based model can simulate the alpha echo (Jansen & Rit, 1995; Vanrullen & MacDonald, 2012). (**A**) Simulation result of the visual evoked potential. (**B**) Experimental data of visual TRF.